First-principles study of the electronic, optical, and lattice vibrational properties of AgSbTe$_2$

Lin-Hui Ye,[1] Khang Hoang,[2] A. J. Freeman,[1] S. D. Mahanti,[2] Jian He,[3] Terry M. Tritt,[3] and M. G. Kanatzidis[4]

[1]*Department of Physics and Astronomy, Northwestern University, Evanston, Illinois 60208, USA*

[2]*Department of Physics and Astronomy, Michigan State University, East Lansing, Michigan 48824, USA*

[3]*Department of Physics and Astronomy, Clemson University, Clemson, South Carolina 60208, USA*

[4]*Department of Chemistry, Northwestern University, Evanston, Illinois 60208, USA*

First-principles calculations of the electronic, optical, and lattice vibrational properties of AgSbTe$_2$ were performed with the generalized gradient approximation (GGA) and the screened-exchange local-density approximation (sx-LDA) method, which successfully corrects the band-gap problem found with GGA. We find a vanishing density of states at the Fermi level, which is consistent with the semiconducting behavior of AgSbTe$_2$. Various optical properties, including the dielectric function, absorption coefficient, and refractive index, as functions of the photon energy are also calculated with the sx-LDA and are found to be in good agreement with experiments. Phonon spectra obtained by the cumulant force constant method show that the optic modes of AgSbTe$_2$ are very low in frequency and should scatter strongly with acoustic modes during heat transport. The calculated specific-heat curve is in general agreement with experiment. Ag/Sb disorder is expected to have a small effect on the electrical transport but may introduce strong phonon scattering due to the large force constant disorder. The scattering of acoustic phonons by optic modes and the possible Ag/Sb disorder may explain the extremely low lattice thermal conductivity of AgSbTe$_2$.

I. INTRODUCTION

AgSbTe$_2$ is the end member of AgPb$_m$SbTe$_{m+2}$ (LAST-m; LAST stands for lead antimony silver tellurium)[1] and similar quaternary systems which are excellent candidates for high-temperature thermoelectrics. Single-phase AgSbTe$_2$ by itself has a large Seebeck coefficient of about 200 μV/K (Refs. 2 and 3) and an extremely low lattice thermal conductivity of about 0.6 W m^{-1} K^{-1}.[3,4] More often, however, it is used to produce composite materials with enhanced energy conversion efficiencies. Combinations of AgSbTe$_2$-AgBiTe$_2$, AgSbTe$_2$-PbTe, and AgSbTe$_2$-SnTe have been studied as early as the 1960s.[2] The so-called TAGS (Te/Ag/Ge/Sb) material, which is one of the commercial products, is made of AgSbTe$_2$ and GeTe. Recently, an exciting discovery was made on the LAST-m family, which have a surprisingly high thermoelectric figure of merit (denoted as ZT).[1] For $m=18$, LAST-m achieves the highest $ZT=1.7$ at 770 K, outperforming all the known bulk thermoelectric materials. In addition, other composites of AgSbTe$_2$ such as Ag(Pb$_{1-y}$Sn$_y$)$_m$SbTe$_{2+m}$ are also found to have good thermoelectric properties.[5]

Although discovered as early as 50 years ago,[6] many physical properties of AgSbTe$_2$ still remain unknown or not well understood. Its crystal structure has been identified to be the disordered NaCl type, with Ag and Sb occupying the sodium sites randomly.[7] However, more recent x-ray and electron-diffraction experiments[8] claim a certain degree of Ag and Sb atomic ordering: Lower symmetries of $P4/mmm$ or $R\bar{3}m$ are found to fit the experimental spectra much better than $Fm\bar{3}m$, which should be the right symmetry if the Ag and Sb occupations are indeed completely random. The electronic structure has been recently calculated[9] by density-functional theory with the generalized gradient approximation (GGA). However, the GGA result is in obvious contradiction with experiments, since it predicts AgSbTe$_2$ to be a good semimetal with bipolar conductivity, while experiments have long established AgSbTe$_2$ to be a degenerate semiconductor with p-type conductivity from both the measured Hall and Seebeck coefficients.[2,3]

Although the origin of the p-type conductivity has not been identified, the wrong density of states (DOS) (Ref. 9) from GGA is not unexpected, since it has been known that local forms of the exchange-correlation potential such as local-density approximation (LDA) or GGA cannot really reproduce the band gaps, due to their rigorous lack of the derivative discontinuity at integer electron numbers.[10] This band-gap problem may be circumvented, for example, by adapting some nonlocal forms of the exchange-correlation potential. Besides, the extremely low lattice thermal conductivity of AgSbTe$_2$ remains a puzzle. There has been no explanation since neither its phonon spectra nor the governing phonon scattering mechanisms are known.

In this paper, we investigate the electronic, optical, and lattice vibrational properties of AgSbTe$_2$ by highly precise first-principles calculations of its ground state with GGA (Ref. 11) and excited-state properties by the screened-exchange LDA (sx-LDA) method,[12] which describes better many semiconductors and insulators. Our calculations confirm the vanishing DOS of AgSbTe$_2$ at the Fermi level and they are therefore consistent with the observed semiconducting behavior of AgSbTe$_2$. We also calculate various optical properties by sx-LDA and show that they are in good agreement with experiments. Finally, the phonon dispersions of AgSbTe$_2$ are calculated by the cumulant force constant method[13] and the specific heat determined from the theoretical phonon spectra is compared with our measured values up to $T=350$ K.

II. STRUCTURAL MODEL AND CALCULATION METHODS

It is still under debate whether the Ag and Sb occupations in AgSbTe$_2$ are ordered or completely random. Possible ordered structures were checked in a previous work,[9] where the AF-IIb structure (space group $F\bar{3}dm$) is identified to be the one with the lowest total energy. This structure is adapted in all our calculations. We realize that the accuracy of the total energy by GGA needs attention due to the obvious band-gap problem in AgSbTe$_2$. However, since it is an integrated quantity over the full Brillouin zone (BZ), the total energy should not be very sensitive to the eigenvalue errors in a small portion of the BZ. Especially, when comparing the relative stability of various structures, this total energy error should largely cancel out. Besides, we point out that since Ag and Sb are not identical elements, some atoms in AgSbTe$_2$ will be displaced from the ideal NaCl lattice sites. Here, all the atomic coordinates are determined by structural optimization and the result shows that it is the Te atoms which are displaced, while Ag and Sb always stay at their exact lattice sites.

For all our calculations, we employ the highly precise all-electron full-potential linearized augmented plane-wave (FLAPW) method.[14] In this method, there is no shape approximation to the charge densities or the potential. It is therefore very appropriate to treat heavy elements such as Ag, Sb, and Te in AgSbTe$_2$, which may be tricky for the pseudopotential method. The muffin-tin radii of Ag, Sb, and Te are chosen to be 2.0, 2.6, and 2.6, respectively. The plane-wave cutoff is chosen as $|\mathbf{k}+\mathbf{G}|<4.0$ and the star-function cutoff as 9.0. All units are in a.u. Integration in the BZ is replaced by summation over the special $\mathbf{k}$ point $3\times3\times3$ Monkhorst–Pack mesh after a careful convergence testing of the $\mathbf{k}$-point mesh is performed. As to the exchange-correlation potential, two schemes are used: the electronic structure and the optical properties are calculated by sx-LDA to ensure the correct eigenvalues. For phonon and specific-heat calculations, we use GGA since our implementation of sx-LDA does not allow the calculation of total energy or forces. Errors from GGA which are included in our phonon and specific-heat results will be discussed.

III. ELECTRONIC STRUCTURE

As is known, one of the origins of the band-gap problem is that the Kohn–Sham gap, when evaluated with the local forms of the exchange-correlation potential such as LDA or GGA, is smaller than the real gap by a value corresponding to the derivative discontinuity of the exchange-correlation potential. It has been shown that using nonlocal exchange can automatically include such a discontinuity and therefore improve the band gap. In the sx-LDA method, the local LDA exchange potential is replaced by the nonlocal Fock exchange operator, which is screened by Thomas–Fermi screening. Without any screening, the sx-LDA method would go back to the well-known Hartree–Fock method which overestimates the band gap. Therefore, the sx-LDA method is one which lies between LDA (which underestimates the
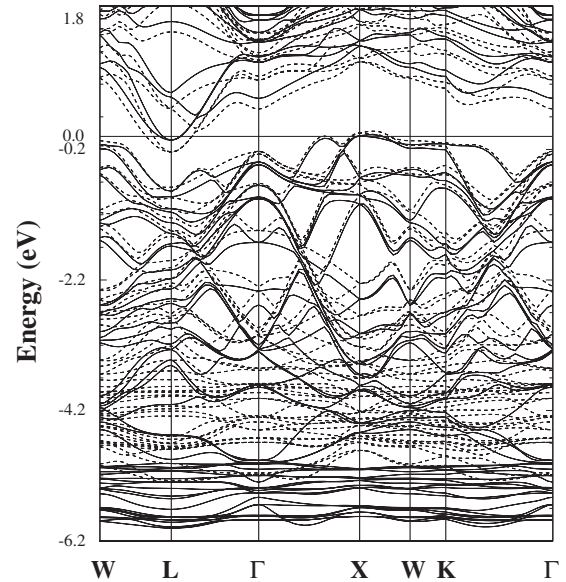
FIG. 1. Band structures of AgSbTe$_2$ by GGA (dashed lines) and sx-LDA (solid lines). The effect of spin-orbit coupling is included in both calculations.

band gap) and Hartree–Fock (which overestimates the band gap). The value of the band gap is thus crucially dependent on the way electron screening is included. Since Thomas–Fermi screening is supposed to work reasonably well for electrons in extended states, it is not surprising to see the many successes of sx-LDA to improve the band gaps by LDA or GGA.

We show in Figs. 1 and 2, respectively, the band structure and the projected density of states (PDOS) obtained in the GGA and sx-LDA calculations. Spin-orbit coupling has been included in the second variational way in these calculations. The two PDOSs in Fig. 2 share similar features, such as that the valence-band top is composed mostly of Te 5p, while the conduction-band bottom is Ag 5s and Sb 5p. In the GGA band structure, the valence-band top has a large overlap ($\sim$0.3 eV) with the conduction-band bottom, which (wrongly) predicts AgSbTe$_2$ to be a good semimetal.[9] On the other hand, such an overlap is almost completely removed by sx-LDA: With the inclusion of the derivative discontinuity of the exchange potential, the valence bands are downshifted, while the conduction bands are upshifted. Consequently, the DOS at the Fermi level (E_F) becomes vanishing and the remaining overlap between the valence-band top and the conduction-band bottom is only about 10 meV. We emphasize that such a tiny energy overlap is beyond the accuracy range of the sx-LDA method which does not mean the absence of a band gap in AgSbTe$_2$. In fact, the vanishing DOS at E_F by the sx-LDA is consistent with experiments which identify AgSbTe$_2$ to be a semiconductor with a very small fundamental band gap.[15]

In Fig. 2, moderate hybridization is seen between Te 5p and Sb 5p in the valence states. However, these hybridizations mostly occur in a deep energy range (i.e., more than 2 eV below E_F). For states close to the valence-band top, the Te-Sb hybridization becomes much weaker. Besides, for Te 5p and Ag 4d, the GGA PDOS seems to show stronger
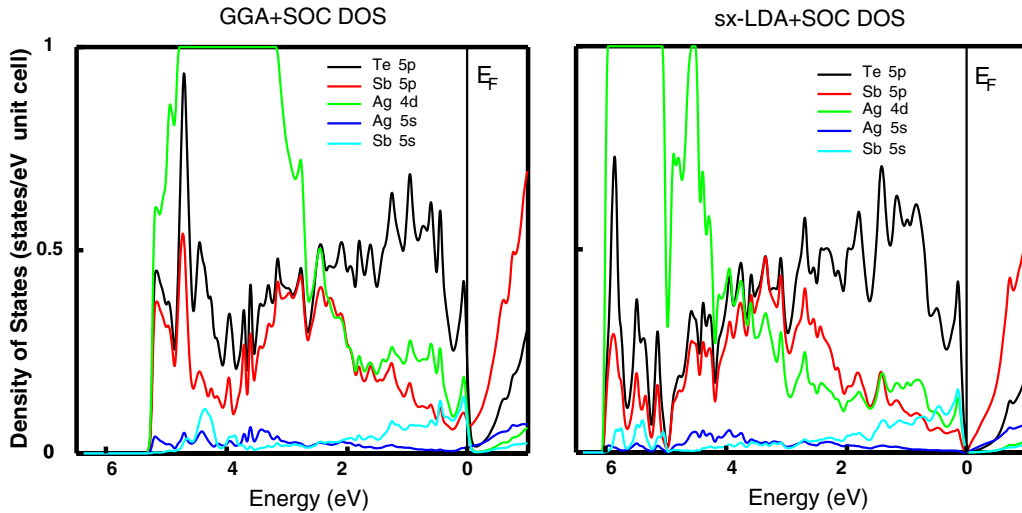
FIG. 2. (Color online) PDOS of AgSbTe$_2$ by GGA (left) and by sx-LDA (right). The effect of spin-orbit coupling is already included in both calculations.

hybridization than Te-Sb. However, the Te-Ag hybridization is apparently overestimated because of the self-interaction error which pushes the Ag 4d too high in energy. In fact, after the self-interaction correction by sx-LDA, a large portion of the Ag 4d PDOS is downshifted to lower energy, which reduces the Te-Ag hybridization for shallow valence states. Especially, the Ag 4d contribution to the valence-band-top states becomes very small.

Two facts can be inferred from the PDOS in Fig. 2: On one hand, the Te-Sb and Te-Ag covalence in deep valence states means that they have some contribution to the total cohesive energy. On the other hand, the fact that the valence-band-top states have a small contribution from either Ag or Sb implies that the carrier dynamics may not be very sensitive to possible Ag or Sb disorder.

IV. OPTICAL PROPERTIES

We now turn to the optical properties which are also calculated by sx-LDA. The comparison of the calculated optical properties with experiments allows us to test the validity of our sx-LDA band structure. With the methods described in Ref. 16, the sx-LDA eigenvalues and eigenvectors are used to construct the real and imaginary parts of the dielectric function, the absorption coefficient, and the refractive index as functions of the photon energy. We present these results in Figs. 3 and 4. Here, we point out that only direct transitions which conserve the crystal momentum are included in our optical property calculations. Indirect transitions such as those assisted by phonons are found to have a very small effect on the absorption edge. In fact, we have compared the absorption spectra by keeping the crystal momentum conservation condition and by relaxing it. The change of the spectral shape around the absorption edge is barely discernible. The weakness of indirect transitions prior to the absorption edge is related to the low DOS of the highly dispersive conduction bands close to the conduction band minimum (CBM).

All the calculated optical properties have been measured with film samples.[17] We first consider the optical gap. Experimentally, it is found to be film thickness dependent. Although the bulk value is not known, when the film thickness increases to 50 nm, the optical gap gradually converges to a value of 0.75 eV. This value is in excellent agreement with our theoretical value of the absorption edge, which is around 0.7–0.8 eV, as can be seen in the inset of Fig. 4(a). Although the experiment assigns this optical gap to indirect transitions, our calculation clearly shows that it comes from direct transitions and that the contribution from indirect transitions to the absorption edge is very weak, as already explained above. We realize, however, that complexities in the interpretation of the optical gap may arise if defects are present. This is likely to be the case for AgSbTe$_2$ since single-phase AgSbTe$_2$ is known to be unstable, and second phases such as Ag$_2$Te and Sb$_2$Te$_3$ are easy to precipitate. If defect states contribute appreciably to intragap excitations, the measured absorption edge will lie within the optical gap. This might be the reason for the smaller gap value of 0.436 eV obtained in another measurement.[18] However, the agree-
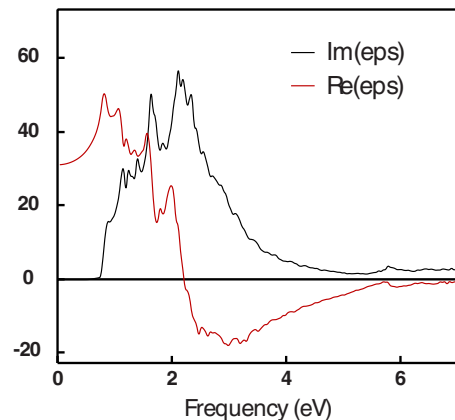
FIG. 3. (Color online) The real and imaginary parts of the dielectric function of AgSbTe$_2$ calculated by sx-LDA.
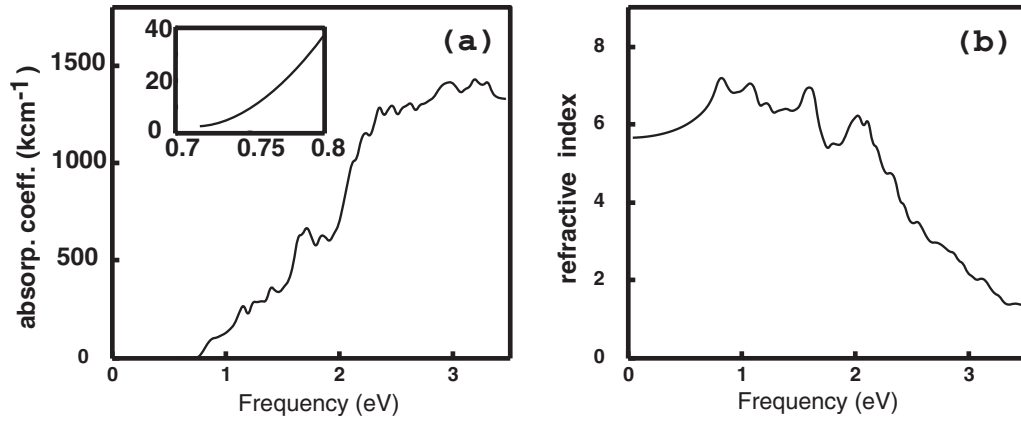
FIG. 4. (a) The absorption coefficient α and (b) the refractive index n as functions of photon energy calculated by sx-LDA. The inset in panel (a) shows that the theoretical absorption edge is located at about 0.70–0.80 eV.

ment between the theoretical absorption edge in Fig. 4 and the measured optical gap of the film samples strongly implies that our sx-LDA band structure is correct.

Further support for our sx-LDA band structure comes from a comparison of other optical properties.[17] Consider the calculated dielectric function in Fig. 3; the main peak of the imaginary part is located at about 2.0 eV, while that of the real part is at about 1.5 eV. These values are both in very good agreement with the measured relative permittivity and the dielectric loss. Moreover, the experimental absorption coefficient reaches a plateau at around 3.0 eV. This feature is also well reproduced by our calculated spectra in Fig. 4. Finally, the measured refractive index achieves a maximum at around 1.5 eV, which matches the theoretical peak position, although the theoretical peak is much broader than the measured one. In general, all the sx-LDA calculated optical properties are in good agreement with experiments.

V. VIBRATIONAL PROPERTIES

The phonon spectra of $AgSbTe_2$ is calculated by the cumulant force constant method based on the harmonic approximation. A special feature of this method is that it does not truncate the long-range atomic interaction, as is usually done in the conventional interatomic force constant method. These two types of force constants are different, but become close in value when the size of the supercell is big enough or the interatomic interactions decay reasonably fast. For $AgSbTe_2$, we tested the phonon calculations with two different supercells: a smaller one with 16 atoms (which is in fact the primitive cell) and a larger one with 64 atoms. The final phonon dispersions are very similar for the two cases, with the difference being that only a few optical bands have slightly higher frequencies for the smaller supercell. We find that this small difference does not affect the following discussion.

The phonon dispersions calculated with the 64-atom supercell are presented in Fig. 5. We need to point out that we have neglected the nonanalytical term of the dynamical matrices which comes from the coupling of the LO modes with the long-range dipolar Coulomb field. This term, which is the

origin of the LO/TO splitting, will affect only the LO modes in a small portion of the BZ centered at Γ. As is well known, it hardly changes the numerical value of various thermodynamic properties such as the entropy, the internal energy, and the specific heat, since these quantities are obtained by integration within the full BZ.

The most obvious feature of Fig. 5 is that the frequencies of the optic modes are very low (although an underestimation of their frequencies may be present; see further discussions in the following). In fact, most optic modes are limited to a small frequency range of $40-80$ cm^{-1}. The softness of the optic modes is partly due to the heavy atomic masses of Ag, Sb, and Te, but it also reflects the relative weak chemical bonds between Te $5p$ and Ag semicore $4d$ and between Te $5p$ and Sb $5p$ states. Also, electrostatic interactions, which contribute to the Madelung term of the cohesive en-
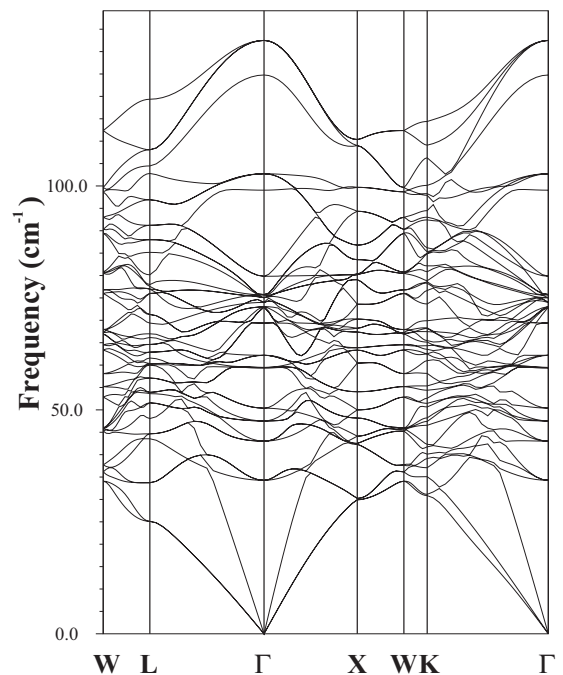
FIG. 5. The phonon dispersions of $AgSbTe_2$ calculated with GGA and the 64-atom supercell.
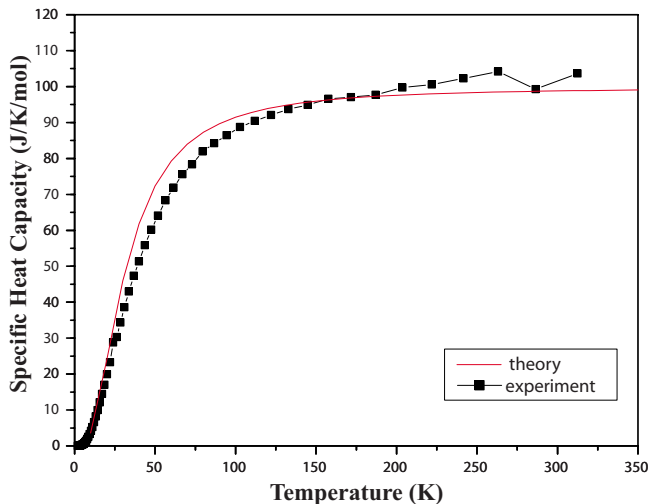
FIG. 6. (Color online) Theoretical and experimental specific heat. Note the theoretical curve is for C_v, while the measured data are C_p.

ergy, should not be strong due to the large anion-cation distances (the Te-Ag and Te-Sb nearest-neighbor distances are both about 3.05 Å). Consequently, the on-site diagonal force constants of Ag, Sb, and Te are only 2.16, 4.72, and 4.08 (units in $\times 10^4$ dyn/cm), respectively, showing that these atoms are only weakly bound to the AgSbTe$_2$ lattice. Especially, the Ag binding is the weakest, which implies that the formation of an Ag vacancy is energetically easy and therefore may be the source of the p-type carriers. However, the real origin of the p-type carriers in AgSbTe$_2$ cannot be determined until other possibilities such as excess Ag are checked by extensive defect calculations.

The closeness between the frequencies of the optic modes and the acoustic modes means that energy transfer between these modes is easy. As a result, with anharmonic effects, acoustic modes which carry the heat flow will be strongly scattered by these low-frequency optic modes. This should be one of the reasons for the extremely low lattice thermal conductivity of AgSbTe$_2$.[3,4]

With this knowledge of the phonon spectra over the full BZ, the lattice vibration contribution to various thermodynamic properties can be calculated. The specific-heat (C_p) measurement was taken on a Quantum Design physical property measurement system relaxation-time calorimeter from 1.8 to 308 K, and the results are compared to the theoretical C_v in Fig. 6. Except for the intrinsic difference between C_v and C_p, the agreement between theory and experiment is medium. The major discrepancy is that the theoretical C_v curve saturates earlier with increasing temperature than the C_p experiment. Although there may be multiple reasons for this discrepancy, one possibility is that some optic-mode frequencies are underestimated by GGA as the saturation of the specific-heat curve will shift to higher temperature if some phonon DOS is extended to higher frequencies.

It is easy to understand why some phonon frequencies may be underestimated by GGA. The origin is related to the band-gap problem: Since the conduction band bottom is too low in energy and overlaps with the valence-band top, some

charges are (wrongly) transferred to Ag and Sb sites from Te sites by GGA. The overpopulation of the Ag 5s and Sb 5p reduces the ionicity of AgSbTe$_2$; i.e., the effective chemical valence of Te becomes less than -2 and those of Ag and Sb become less than $+1$ and $+3$, respectively. The weakening of the electrostatic interactions thus leads to the underestimation of the phonon frequencies. This frequency error can only be corrected with other methods which can avoid the band-gap problem in both the calculations of the forces and the band structure. However, the general agreement of the specific heat between theory and experiment in Fig. 6 implies that the major features of the phonon spectra are still well reproduced in Fig. 5.

VI. DISCUSSION AND CONCLUSION

As an important material for thermoelectric applications, many physical properties of AgSbTe$_2$ had not been well studied. In this work, we have calculated the electronic, optical, and lattice vibrational properties of AgSbTe$_2$ by a highly precise first-principles method. Our sx-LDA calculations within FLAPW show that the wrong (semi)metallic DOS by GGA is clearly due to the band-gap problem. Inclusion of the derivative discontinuity of the exchange potential by sx-LDA results in a band structure which has a vanishing DOS at the Fermi level, which is consistent with experiment. The correctness of the sx-LDA band structure is further supported by the good agreement between the calculated optical properties and experiment. A major feature of the phonon spectra, namely, most optic modes are low in frequency, implies strong scattering of the acoustic modes by these optic modes. This should be one of the reasons for the extremely low lattice thermal conductivity of AgSbTe$_2$.

We now consider the effects of possible Ag/Sb disorder. In the NaCl structure, every Ag is bound to six nearest-neighbor Te, forming an Ag-centered octahedron. This is also the case for Sb. The major complexity of the AgSbTe$_2$ structure comes from the Te-centered octahedra. Ideally, each Te is bound to three Ag and three Sb, which ensures the local charge balance in the octahedron. If by disorder some Ag exchange their positions with Sb so that some Te-centered octahedra have excess Ag and some others have excess Sb, then the violation of local charge balance will cause a large cohesive energy loss. Such disordered structures are not likely to be stable, which may explain why the structure AF-I is much higher in energy than AF-IIb and AF-III in Ref. 9. Therefore, for the stable structures of AgSbTe$_2$, we assume that most Te-centered octahedral have three Ag and three Sb.

Within one Te-centered octahedron, the three Ag and the three Sb can occupy the six nearest-neighbor sites of the Te in different ways, all of which maintain local charge balance. Our concern is how such disorder can affect the electric carriers (holes) and the heat carriers (phonons). We believe that the effect of Ag/Sb disorder on the holes is small mainly because of two reasons. First, since the Te 5p shell is completely filled, the valence-band-top states are rather isotropic and are therefore less affected by local atomic disorder, which is very similar to the situation of amorphous semiconductors.[19] Moreover, our sx-LDA PDOS has shown

that the valence-band-top states actually have a very small contribution from Ag and Sb. This feature further reduces the sensitivity of the holes to the Ag/Sb disorder.

The effect of the same Ag/Sb disorder on phonons is very different from that on the holes since they are governed by completely different factors. The scattering of phonons is through the atomic mass disorder and force constant disorder. Although the atomic masses of Ag and Sb are similar, their force constants are very different; as shown in the above, the on-site diagonal force constant of Ag is less than half of that of Sb. Such a big difference in the force constants reflects the very different nature of the Te-Ag and the Te-Sb bonds. However, it is probable that, to a larger extent, it is due to the different ionic charges of Ag^{1+} versus Sb^{3+}. Phonon scattering should be strong in $AgSbTe_2$ with such force constant disorder. This might be another reason for the extremely low lattice thermal conductivity. Combined with the above argument about the effect of the disorder on electrical transport, one expects that the Ag/Sb disorder in the cation sublattice is favorable to the thermoelectric properties of $AgSbTe_2$.

[1] K. F. Hsu, S. Loo, F. Guo, W. Chen, J. S. Dyck, C. Uher, T. Hogan, E. K. Polychroniadis, and M. G. Kanazidis, Science **303**, 818 (2004).

[2] T. Irie, T. Takahama, and T. Ono, Jpn. J. Appl. Phys. **2**, 72 (1963).

[3] R. Wolfe, J. H. Wernick, and S. E. Haszko, J. Appl. Phys. **31**, 1959 (1960).

[4] E. F. Hockings, J. Phys. Chem. Solids **10**, 341 (1959).

[5] J. Androulakis, K. F. Hsu, R. Pcionek, J. Kong, C. Uher, J. J. D'angelo, A. Downey, T. Hogan, and M. G. Kanatzidis, Adv. Mater. (Weinheim, Ger.) **18**, 1170 (2006).

[6] J. H. Wernick and K. E. Benson, J. Phys. Chem. Solids **3**, 157 (1957); J. H. Wernick, S. Geller, and K. E. Benson, *ibid.* **4**, 154 (1958)

[7] S. Geller and J. H. Wernick, Acta Crystallogr. **12**, 46 (1959).

[8] E. Quarez, K.-F. Hsu, R. Pcionek, N. Frangis, E. K. Polychroniadis, and M. G. Kanatzidis, J. Am. Chem. Soc. **127**, 9177 (2005).

[9] K. Hoang, S. D. Mahanti, J. R. Salvador, and M. G. Kanatzidis, Phys. Rev. Lett. **99**, 156403 (2007).

[10] J. P. Perdew, R. G. Parr, M. Levy, and J. L. Balduz, Jr., Phys. Rev. Lett. **49**, 1691 (1982).

[11] J. P. Perdew, K. Burke, and M. Ernzerhof, Phys. Rev. Lett. **77**, 3865 (1996).

[12] A. Seidl, A. Görling, P. Vogl, J. A. Majewski, and M. Levy, Phys. Rev. B **53**, 3764 (1996).

[13] K. Parlinski, Z.-Q. Li, and Y. Kawazoe, Phys. Rev. Lett. **78**, 4063 (1997).

[14] E. Wimmer, H. Krakauer, M. Weinert, and A. J. Freeman, Phys. Rev. B **24**, 864 (1981); H. J. F. Jansen and A. J. Freeman, *ibid.* **30**, 561 (1984).

[15] Recent transport measurements reveal that the fundamental band gap of $AgSbTe_2$ is as small as a few meV [V. Jovovic and J. P. Heremans, Phys. Rev. B (to be published)].

[16] S. H. Rhim, M. Kim, A. J. Freeman, and R. Asahi, Phys. Rev. B **71**, 045202 (2005).

[17] H. A. Zayed, A. M. Ibrahim, and L. I. Soliman, Vacuum **47**, 49 (1996); A. Abdelghany, S. N. Elsayed, A. H. Abou El Ela, and N. H. Mousa, *ibid.* **47**, 243 (1996).

[18] S. N. Elsayed, A. Abdelghany, A. H. Abou El Ela, and N. H. Mousa, Phys. Chem. Liq. **28**, 165 (1994).

[19] T. Kamiya, S. Narushima, H. Mizoguchi, K. Shimizu, K. Ueda, H. Ohta, M. Hirano, and H. Hosono, Adv. Funct. Mater. **15**, 968 (2005).